TM No.
316-489-76

NAVAL UNDERWATER SYSTEMS CENTER
NEW LONDON LABORATORY
NEW LONDON, CONNECTICUT 06320

Technical Memorandum

A NEARFIELD MODEL OF THE PARAMETRIC RADIATOR.
PART III, CONVOLUTION METHOD *

19 October 1976

Prepared by:

R. H. Mellen
Advanced Systems
Technology Division

M. B. Moffett
Sonar Transducers and
Arrays Division

80   4 28 008

ABSTRACT

The line array solution of Part I is used in convolution with the primary pattern to calculate the field of collimated and spherically diverging sources of arbitrary transverse distribution.

ADMINISTRATIVE INFORMATION

INTRODUCTION

In Part I (reference (1)) the contour integration method was used to calculate the field of a line array. On the axis the solution has a logarithmic singularity. Finite aperture axial levels were calculated for two special cases: a cylindrical and a conical source in which the transverse densities are constant within the aperture and zero outside. A "complete" field solution for each case is now obtained in which the transverse distributions can be arbitrary. The solution is in the form of a convolution between the line array pattern and the source pattern. This is equivalent to summing the fields of a bundle of line arrays of appropriate weights.

CYLINDRICAL SOURCE

The volume integral for the cylindrical source can be written

$$\psi(\vec{R}) = \frac{Q_0 \exp(-\alpha L - ikL)}{4\pi} \int_0^{2\pi} d\gamma' \int_0^\infty a'da' D(a',\gamma') \int_{-L}^\infty \frac{dx \exp\left[-2\alpha x - ik(\sqrt{x^2 + a_1^2} + x)\right]}{\sqrt{x^2 + a_1^2}} \tag{1}$$

Where ψ is the velocity potential, Q_0 is the linear source density, $\vec{R}$ is the range vector to the field point and $a_1^2 = a^2 + a'^2 - 2aa' \cos(\gamma' - \gamma)$ where γ is the cylindrical angle of the radius a'. $D(a',\gamma')$ is the normalized transverse distribution function; i.e.

$$\int_0^{2\pi} d\gamma' \int_0^\infty a'da' D(a',\gamma') \equiv 1 \tag{2}$$

Let $Y = L \psi(L,a)\exp(ikL)/S_0$ where $S_0 = Q_0/4\pi\alpha$ is the Westervelt source strength. Equation (1) can then be written in dimensionless form as

$$Y = \int_0^{2\pi} d\gamma' \int_0^\infty a'da' D(a',\gamma') Y(u_0,v_0) \tag{3}$$

From reference (1)

$$Y(u_0,v_0) = u_0 \exp(-u_0) \int_{z_0}^\infty \frac{dz \exp(-z)}{\sqrt{z^2 + B^2}} \tag{4}$$

5

is the line array solution and where $z + -u_0 + iv_0 \simeq -2\alpha L + ika_1^2/2L$ and $B^2 \simeq 4iu_0v_0$ for $L \gg a$.

Equation (4) is easily evaluated along the contour $z = t - u_0 + iv_0$. Equation (3) is then the two dimensional convolution of Equation (4) and $D(a',\gamma')$.

DIVERGING SOURCE

In the spherical case let $Y = R\psi(\vec{R})\exp(ikR)/S_0$. Equation (3) becomes

$$Y = \int_0^{2\pi} d\gamma' \int_0^{\pi} d\phi' \sin\phi' \, D(\phi',\gamma') \, \exp(iv_0) \, Y(u_0,v_0) \tag{5}$$

where D is the normalized density function; i.e.

$$\int_0^{2\pi} d\gamma' \int_0^{\pi} d\phi' \, \sin\phi' \, D(\phi',\gamma') \equiv 1 \tag{6}$$

and where $Y(u_0,v_0)$ is again given by Equation (4). For small angles $u_0 \simeq 2\alpha R$, $v_0 \simeq u_0\theta_1^2$ and $\theta_1^2 \simeq \theta^2 + \theta'^2 - 2\theta\theta'\cos(\gamma'-\gamma)$ where $\theta' = \phi'/\phi_0$, ϕ_0 being the characteristic Westervelt angle of reference (1). At long ranges $Y(u_0,v_0)$ approaches the Westervelt pattern except for the singularity at $\theta_1 = 0$. Some results of convolution in this limiting case are reported in reference (2).

Equation (5) was programmed for numerical evaluation using the conical beam approximation. The singularity at $\theta_1 = 0$ was avoided by using small finite initial values. The results for various values of $u_0 = 2\alpha R$ are shown in Figures 1 - 3. The scaled conical angle is given by $\theta_0 = \phi_0'/\phi_0$ where ϕ_0' is the half width of the conical beam. The abscissas are the relative angle $\theta = \phi/\phi_0$ as in reference (1). The ordinates are $20 \log_{10} |Y|$. The dotted curve is the Westervelt pattern.

For $\theta_0 = 0$ the conical beam is a delta function and the pattern has a logarithmic singularity given by ($u_0 \ll 1$)

$$Y(u_0,v_0) \rightarrow -u_0 \exp(-u_0) \ln |v_0|$$

$$\theta \rightarrow 0 \tag{7}$$

6

For $\theta_0 \neq 0$, Y rapidly approaches the finite axial value for $\theta < \theta_0$. For $\theta_0 > 1$ the curves cross the $\theta_0 = 0$ curve and approach it from above. For $\theta_0 \rightarrow \infty$ the $\theta_0 = 0$ curve acts like a delta function with respect to the conical beam. It is clear that only for $\theta_0 >> 1$ does the actual shape of the source pattern have any significant effect on the result.

Figure 4 compares the results with experiment where $\theta_0 = 0.4$. For $2\alpha L = 1$ the agreement is good. The -3dB beamwidth is only $\frac{1}{2}$ the Westervelt beamwidth. For $2\alpha L = 0.25$ the experimental axial value is again roughly 3dB low as it was in the calculations of reference (1). Misalignment of source and receiver is one possible explanation of this error.

SATURATION

The effects of saturation may be included as in Part II (reference (3)) by multiplying the integrand of Equation (4) by the taper function $T^2(z)$. The solution for the cylindrical and spherical cases may also be combined to give a reasonably good approximation for all ranges. At moderate range the spherical part alone should give a sufficiently good approximation if the result is multiplied by the source aperture pattern (reference (4)).

REFERENCES

1. R. H. Mellen, "A Nearfield Model of the Parametric Radiator," NUSC Technical Memorandum PA4-230-75, December 1975.

2. H. O. Berktay and D. J. Leahy, "Farfield Performance of Parametric Transmitters," J. Acoust. Soc. Am. 55, 539-546 (1974).

3. R. H. Mellen, "A Nearfield Model of the Parametric Radiator, Part II: Saturated Sources," NUSC Technical Memorandum PA4-53-76, May 1976.

4. M. B. Moffett and R. H. Mellen, "On Parametric Source Aperture Factors," J. Acoust. Soc. Am. 60, 581-583 (1976).
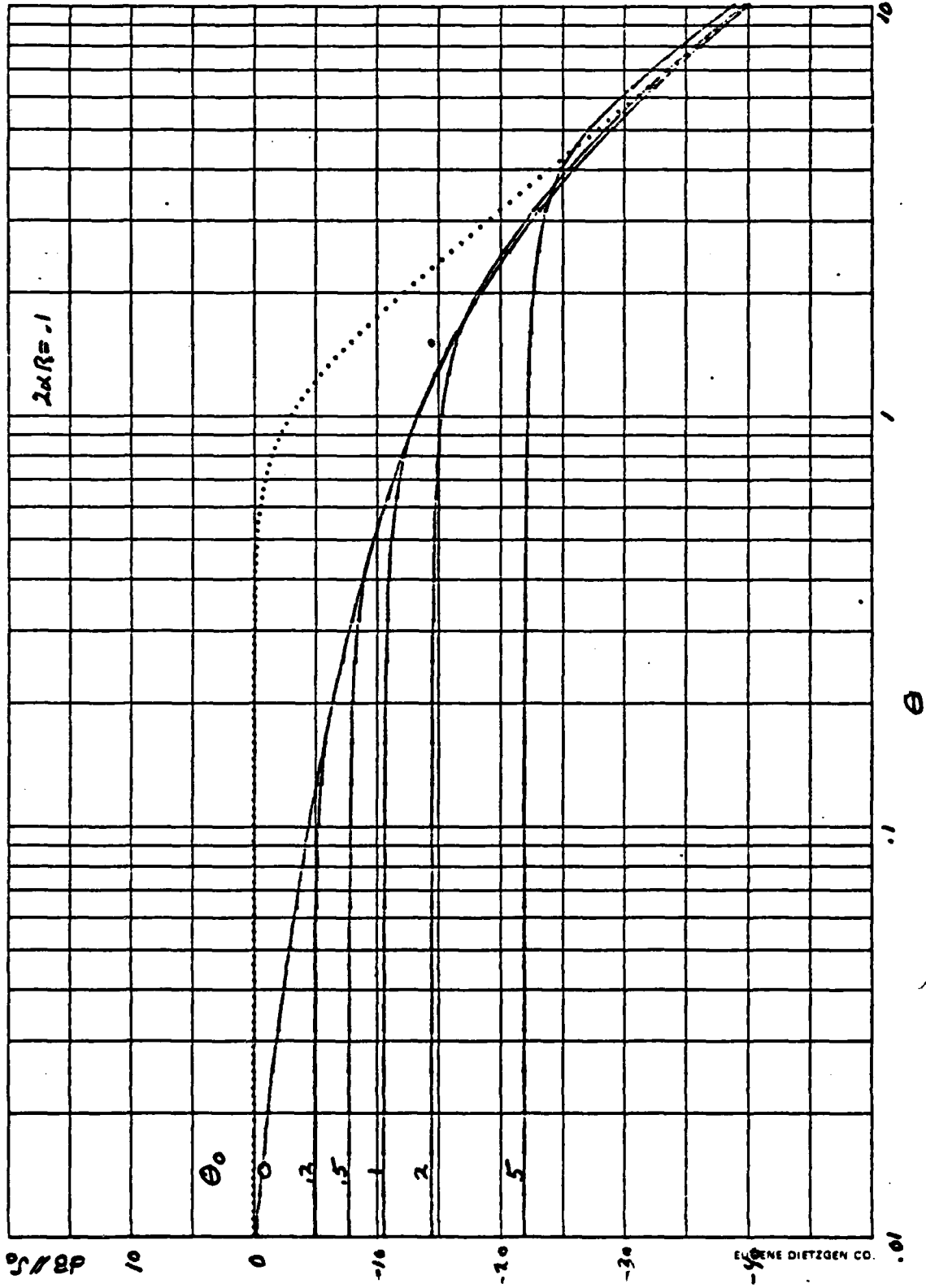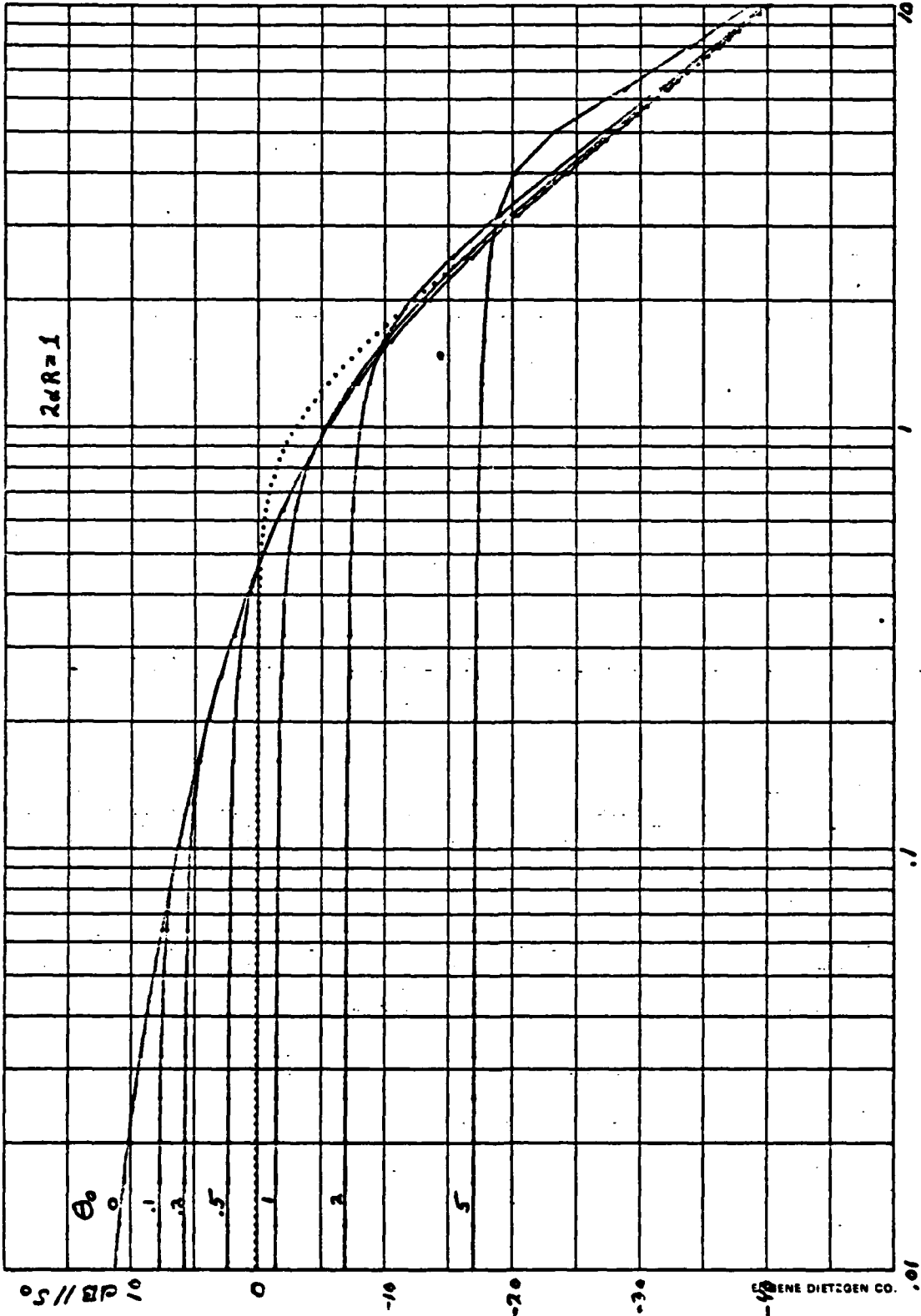
Figure 1.   Beam Pattern $2\alpha R = 0.1$

Figure 2.   Beam Pattern $2\alpha R = 1$

9

Figure 3.   Beam Pattern $2\alpha R = 10$

3ND-NUSC/NL-3900/6 (REV. 2-71) 3 Cycle x 70 Divisions
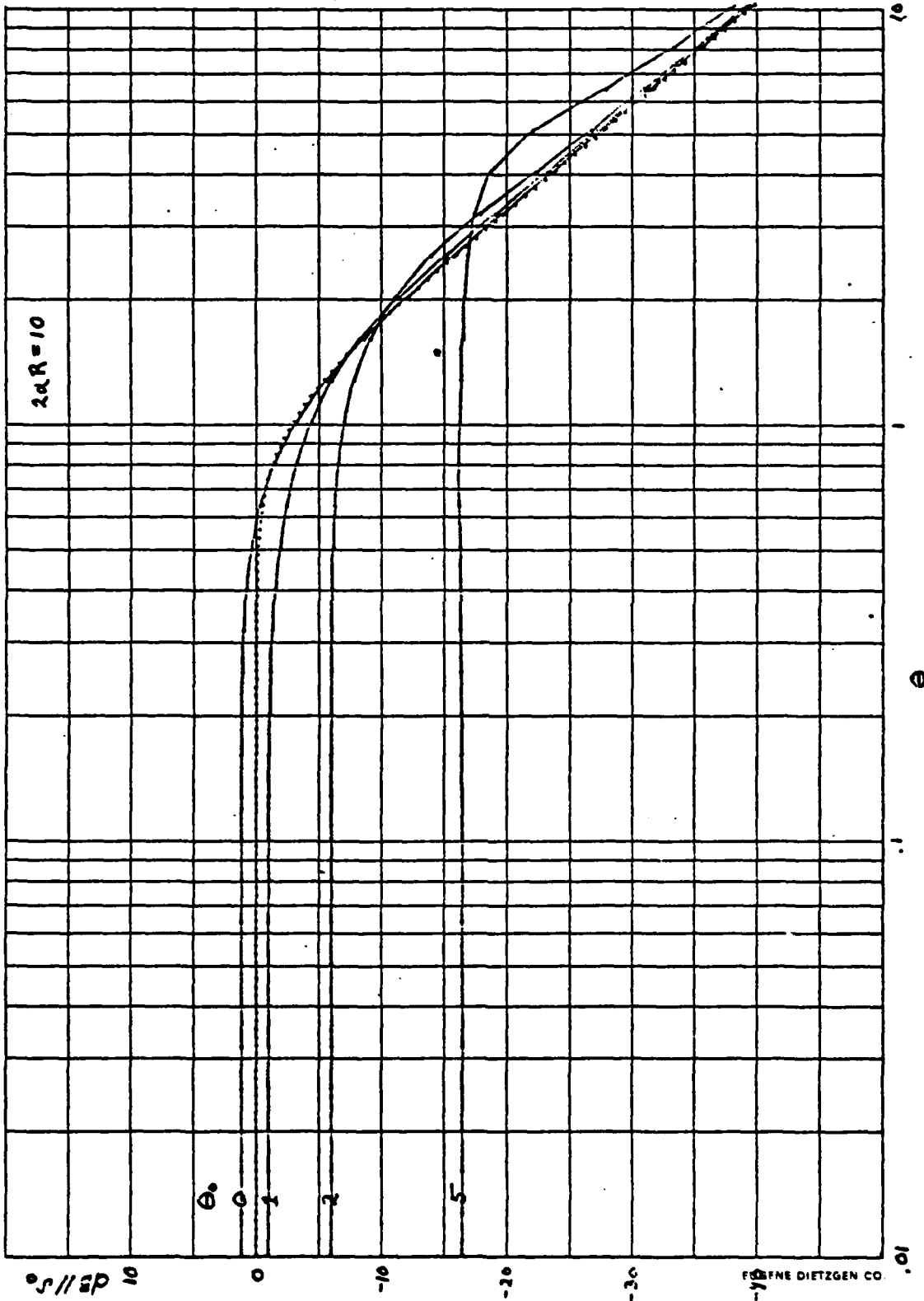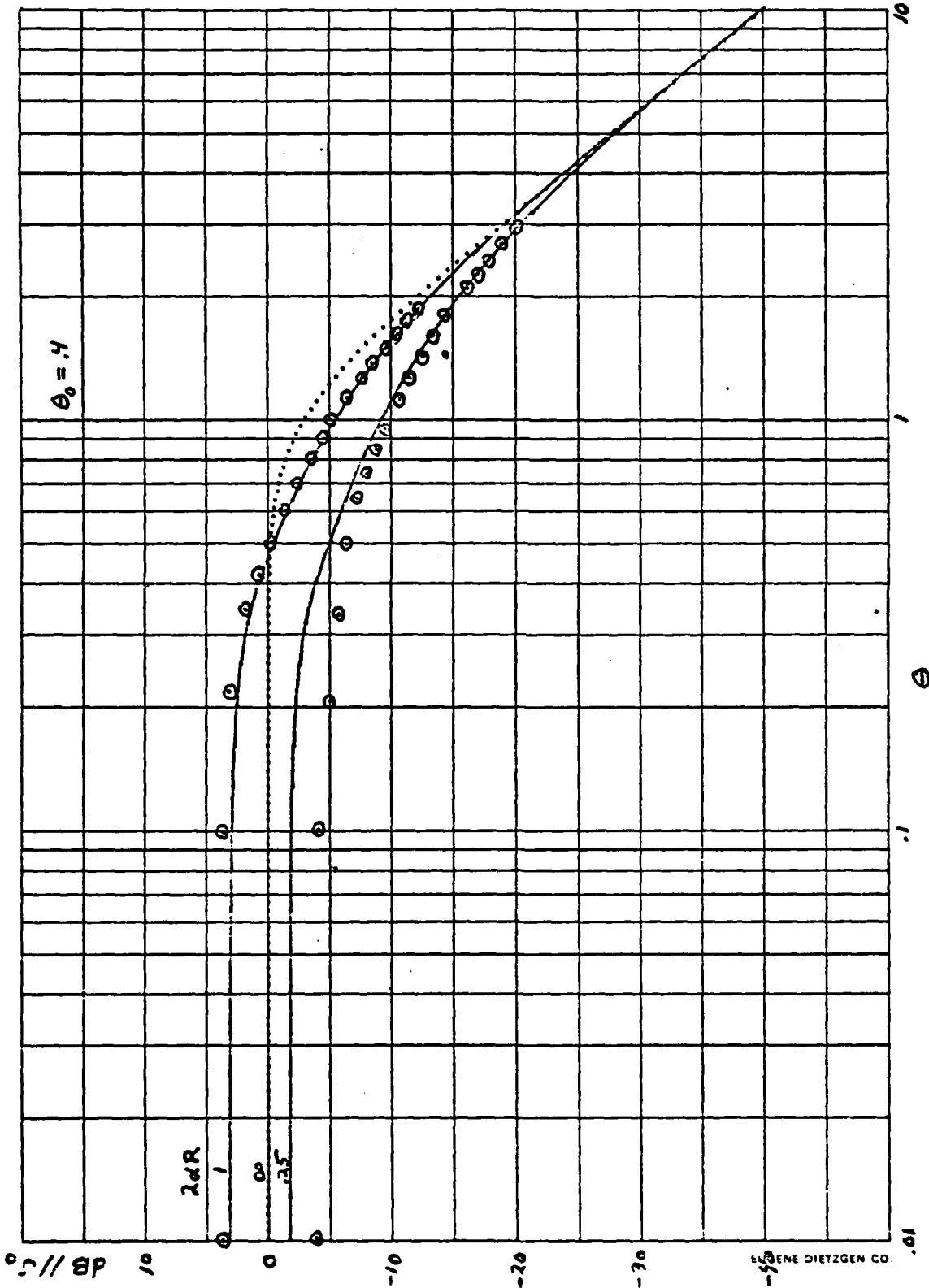

Figure 4. Comparison of experimental and predicted beam patterns.

EUGENE DIETZGEN CO.